

МАТЕРИАЛОВЕДЕНИЕ, МЕТАЛЛУРГИЯ

MATERIALS ENGINEERING, METALLURGY

UDC 539.32;548.526;548.528
<https://doi.org/10.29235/1561-8358-2020-65-2-135-144>

Received 25.03.2020
Поступила в редакцию 25.03.2020

Valeri M. Fedosyuk, Tatiana I. Zubar, Alex V. Trukhanov

*Scientific and Practical Materials Research Center of the National Academy of Sciences of Belarus,
Minsk, Republic of Belarus*

**INFLUENCE OF ELECTRODEPOSITION PARAMETERS ON STRUCTURE
AND MICROMECHANICAL PROPERTIES OF THIN Ni–Fe FILMS**

Abstract. The correlation between the synthesis modes, chemical composition, crystal structure, surface microstructure, and also the mechanical properties of thin nanostructured Ni – Fe films has been studied. Thin Ni–Fe films on the Si with Au sublayer were obtained using electrolyte deposition with different current modes: direct current and three pulsed modes with pulse duration of 1 s, 10^{-3} and 10^{-5} s. It is shown that a decrease in the pulse duration to 10^{-5} s leads to an increase in the film elastic modulus and the hardness due to the small grain size and a large number of grain boundaries with increased resistance to plastic deformation. The effect of heat treatment at 100, 200, 300, and 400 °C on the surface microstructure and micromechanical properties of the films was investigated. An increase in grain size from 6 to 200 nm was found after heat treatment at 400 °C which, in combination with interdiffusion processes of the half-layer material, led to a significant decrease in hardness and elastic modulus. Ni–Fe films with improved mechanical properties can be used as coatings for microelectronic body for their electromagnetic protection.

Keywords: thin Ni–Fe film, electrodeposition, structure, hardness, elastic modulus

For citation: Fedosyuk V. M., Zubar T. I., Trukhanov A. V. Influence of electrodeposition parameters on structure and micromechanical properties of thin Ni–Fe films. *Vesti Natsyunal'noi akademii nauk Belarusi. Seriya fizika-technichnykh nauk = Proceedings of the National Academy of Sciences of Belarus. Physical-technical series*, 2020, vol. 65, no. 2, pp. 135–144. <https://doi.org/10.29235/1561-8358-2020-65-2-135-144>

В. М. Федосюк, Т. И. Зубарь, А. В. Труханов

*Научно-практический центр Национальной академии наук Беларуси по материаловедению, Минск,
Республика Беларусь*

**ВЛИЯНИЕ ПАРАМЕТРОВ ЭЛЕКТРОЛИТИЧЕСКОГО ОСАЖДЕНИЯ НА СТРУКТУРУ
И МИКРОМЕХАНИЧЕСКИЕ СВОЙСТВА ПЛЕНОК Ni–Fe**

Аннотация. Проведены исследования корреляции между режимами синтеза, химическим составом, кристаллической структурой и микроструктурой поверхности, а также механическими свойствами тонких наноструктурированных пленок Ni–Fe. Тонкие пленки Ni–Fe были получены в различных режимах электролитического осаждения: в режиме постоянного тока и в импульсных режимах с длительностью импульса 1 с, 10^{-3} и 10^{-5} с. Показано, что уменьшение длительности импульса до 10^{-5} с приводит к увеличению модуля упругости и твердости пленок благодаря малому размеру зерна и, соответственно, большому количеству границ зерен с повышенным сопротивлением пластической деформации. Исследовано влияние термической обработки при $T = 100, 200, 300$ и 400 °C на микроструктуру поверхности и микромеханические свойства пленок. После термообработки при 400 °C наблюдалось увеличение размера зерна от 6 до 200 нм, что в сочетании с процессами взаимодиффузии материала подслоя и пленки привело к значительному снижению твердости и модуля упругости. Пленки Ni–Fe с улучшенными механическими свойствами могут быть использованы как покрытия корпусов микроэлектроники для электромагнитной их защиты.

Ключевые слова: тонкие пленки Ni–Fe, электролитическое осаждение, структура, механизм роста, механические свойства

Для цитирования: Федосюк, В. М. Влияние параметров электролитического осаждения на структуру и микро-механические свойства пленок Ni–Fe / В. М. Федосюк, Т. И. Зубарь, А. В. Труханов // Вес. Нац. акад. навук Беларусі. Сер. фіз.-тэхн. навук. – 2020. – Т. 65, № 2. – С. 135–144. <https://doi.org/10.29235/1561-8358-2020-65-2-135-144>

Introduction. The development of nanotechnology and the tendency to miniaturization are the main trends of modern scientific and technological progress. Over the past decade, the global market of production and use of thin and nanostructured films has increased by 2–3 times. After applying thin and nanostructured films and coatings, the product surface can acquire new functional properties and, at the same time, its performance characteristics increase [1–3]. Magnetic nanostructured films and separate Ni–Fe nanoparticles are the basis for the development of a new generation of high-density magnetoresistive random access memory, quantum computers, and other topical applications of microelectronics and spintronics [4–6]. In addition, the magnetic properties of nanoparticle ensembles have not yet been sufficiently studied and, therefore, are of interest from fundamental perspective. For example, near the percolation threshold of partially filled nanostructured films, there may occur a magnetic domain structure, ordered in a geometric cluster of single-domain magnetic particles [7]. The appearance of such magnetic structure is due to the peculiarities of the microstructure dipole-dipole and exchange magnetic interactions. In turn, the microstructure features are formed at the stage of film origin and largely depend on the mechanisms of its growth [8–10]. The use of pulsed electrodeposition modes at the synthesis of Ni–Fe nanostructured magnetic films allows controlling the microstructure parameters by controlling the average grain size, the degree of film filling, and the mechanism of its growth, which opens up wide opportunities for the synthesis of films with controlled functional properties [11, 12].

Thus, *the purpose of this work* is to study the effect of the parameters of electrodeposition of thin nanostructured Ni–Fe films on their composition, crystal structure and surface microstructure, as well as on mechanical properties.

Materials and methods of research. Thin Ni–Fe films were synthesized by electrolyte deposition in various modes: stationary electrodeposition (at constant current) and in pulse modes with different pulse durations. The films were deposited on a silicon plate with a crystallographic orientation (100) on a 100 nm thick gold sublayer. Deposition of the films with the desired stoichiometry – Ni₈₀Fe₂₀ – was performed from a standard combined electrolyte composition: NiSO₄ – 210 g/l, NiCl₂ – 20 g/l, H₃BO₃ – 30 g/l, MgSO₄ – 60 g/l, FeSO₄ – 15 g/l, saccharin – 1 g/l. The electrolyte temperature was maintained at 30–35 °C, pH = 2.3–2.5. The current density of $j = 25 \text{ mA/cm}^2$.

The samples of thin Ni–Fe films, obtained by stationary (DC) and pulsed electrodeposition, differed in the pulse duration (t_{on}), which was equal to the pause duration (t_{off}):

- 1) obtained by DC (DC mode), $t_{\text{on}} = t_{\text{full}}$;
- 2) obtained by the long-pulse mode, $t_{\text{on}} = 1 \text{ s}$;
- 3) obtained by the medium pulse mode, $t_{\text{on}} = 1 \text{ ms} = 10^{-3} \text{ s}$;
- 4) obtained by the short-pulse mode, $t_{\text{on}} = 10 \text{ mcs} = 10^{-5} \text{ s}$.

The total electrodeposition time (t_{full}) was 5, 30 and 60 s for each mode. Table 1 provides details of the synthesis modes of nanostructured Ni–Fe films.

The chemical composition of the research objects was studied using Energy-dispersive X-ray spectroscopy (EDX) with spectrometer by Rigaku

Table 1. Features of electrodeposition modes of nanostructured Ni–Fe films obtained with different pulse durations for $t_{\text{full}} = 60 \text{ s}$

Mode	$t_{\text{full}}, \text{ s}$	$t_{\text{on}}, \text{ s}$	$t_{\text{off}}, \text{ s}$	N_u^*	$t_{\text{eff}}, \text{ s}^{**}$
Direct current (DC)	60	60	–	–	60
Long pulse (LP)	60	1	1	30	30
Medium pulse (MP)	60	$1 \cdot 10^{-3}$	$1 \cdot 10^{-3}$	$3 \cdot 10^4$	30
Short pulse (SP)	60	$1 \cdot 10^{-5}$	$1 \cdot 10^{-5}$	$3 \cdot 10^6$	30

* N_u – number of current pulses during the full deposition time.

** t_{eff} – effective time of electrodeposition, $t_{\text{eff}} = t_{\text{on}} N_u$.

Inc. Crystal structure and qualitative phase analysis were performed at room temperature using the DRON-3M X-ray diffractometer (XRD) with CuK $_{\alpha}$ ($\lambda = 0.178 \text{ nm}$) in the range of 10–100° in increments of 0.05°. The crystal structure was evaluated using the Rietveld method using the FullProf.

The surface microstructure was studied using the HT-206 atomic force microscope (AFM) and the Hitachi TM3030 scanning electron microscope (SEM).

Micromechanical parameters were measured using the nanoindenter 750 UBI (Hysitron, USA) by introducing the Berkovich diamond pyramid with continuous registration of deformation curves. For each sample, at least 25 measurements were made in the normal load range from 0.1 to 10 mN. Each deformation curve included 4,000 measurements. Loading of materials was carried out according to the scheme “10–10” (10 s of loading, 10 s of unloading). The Oliver–Farr method was used to calculate micromechanical properties [13]. The calculation of the inter-diffusion process of gold atoms into a Ni–Fe film was carried out according to the basic diffusion equation (I Fick’s law) and the Arrhenius equation [14, 15]. The temperature dependence of the diffusion coefficient was determined by the equation 1:

$$D(T) = D_0 \exp\left[-\frac{Q}{T}\right].$$

Where D_0 – factor of diffusion (cm^2/s), Q – activation temperature of the diffusion process corresponding to the activation energy (J/mol), T – thermodynamic temperature (K). For gold atoms diffusing in the film, $D_0 = 1.01 \cdot 10^{-3} \text{ cm}^2/\text{s}$ and $Q = 17,750 \text{ K}$ [16].

Results and discussion. The results of studies of nanostructured films of the Ni–Fe system using EDX (Fig. 1) showed that the Ni/Fe ratio is not constant for samples obtained using different deposition process modes (DC and pulse modes with different pulse durations). The chemical composition of the electrolyte used for electrodeposition was chosen in a way that the stoichiometric ratio of the synthesized films was close to $\text{Ni}_{80}\text{Fe}_{20}$. This alloy has a high magnetic permeability, low coercive force and close to zero magnetostriction, as well as a significant magnetoresistive effect. The composition of the film obtained in DC mode was as close as possible to the predicted one – $\text{Ni}_{79.39}\text{Fe}_{20.61}$.

Switching to pulsed electrodeposition modes provided a deviation from stoichiometry that changed non-linearly with decreasing pulse duration. Fig. 1, *e* shows the change in the stoichiometric ratio of Ni and Fe in films obtained in different electrodeposition modes at $t_{\text{full}} = 60 \text{ s}$. When switching from DC mode to pulse mode with a pulse duration of 1 s and 10^{-3} s , an increase in the iron content from 20.61 to 24.45 at.% is observed. With a further decrease in the pulse duration and switching to the mode with $t_{\text{on}} = 10^{-5} \text{ s}$, a decrease in the iron concentration to 18.24 at.% was recorded.

The chemical composition gradient, exactly, the increase in the iron content in Ni–Fe films near the substrate with subsequent stabilization of the composition, is a known phenomenon found in binary (Ni–Fe, Co–Ni, Co–Fe) and triple (Co–Ni–Fe) alloys obtained by electrodeposition [17, 18]. The stoichiometric ratio in a binary Ni–Fe alloy is determined by the kinetics of the ion reduction process in the cathode fall region. Changing the technological parameters can cause a significant shift in the equilibrium of the

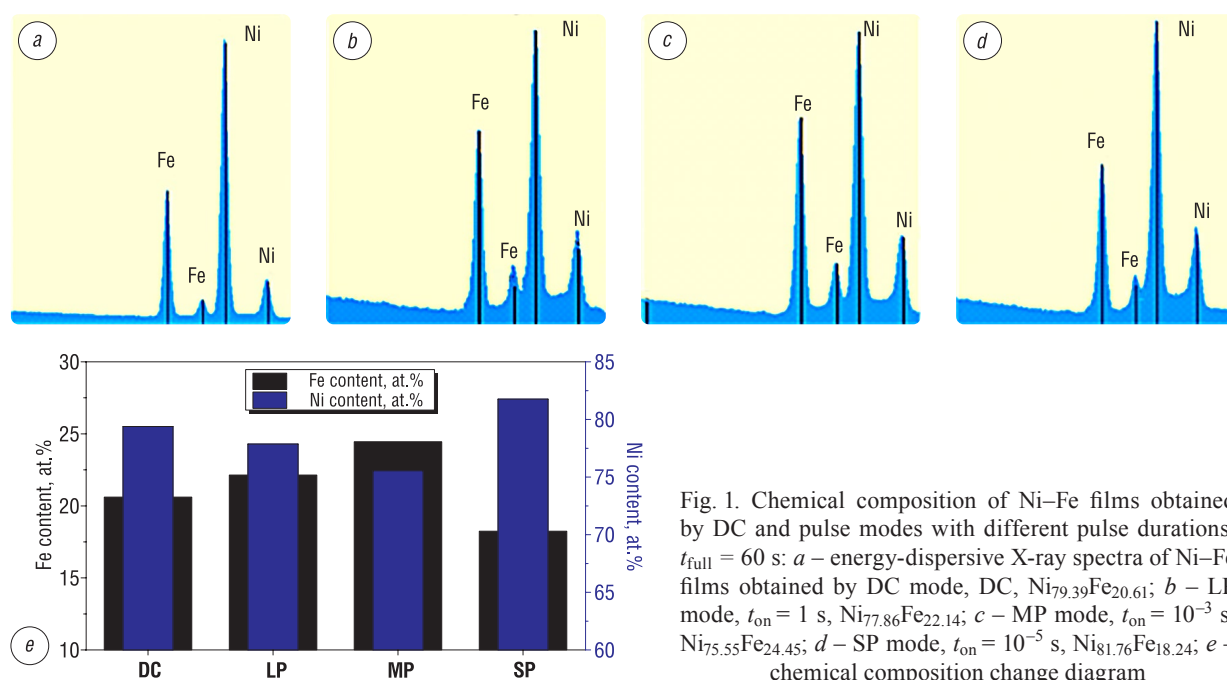


Fig. 1. Chemical composition of Ni–Fe films obtained by DC and pulse modes with different pulse durations, $t_{\text{full}} = 60 \text{ s}$: *a* – energy-dispersive X-ray spectra of Ni–Fe films obtained by DC mode, DC, $\text{Ni}_{79.39}\text{Fe}_{20.61}$; *b* – LP mode, $t_{\text{on}} = 1 \text{ s}$, $\text{Ni}_{77.86}\text{Fe}_{22.14}$; *c* – MP mode, $t_{\text{on}} = 10^{-3} \text{ s}$, $\text{Ni}_{75.55}\text{Fe}_{24.45}$; *d* – SP mode, $t_{\text{on}} = 10^{-5} \text{ s}$, $\text{Ni}_{81.76}\text{Fe}_{18.24}$; *e* – chemical composition change diagram

redox reaction: $\text{Fe}^{2+} + 2\text{e}^- \rightarrow \text{Fe}^0$, which can lead to a substantial deviation from stoichiometry. For example, an increase in the electrolyte temperature above 40–45 °C contributes to the transition of $\text{Fe}^{2+} \rightarrow \text{Fe}^{3+}$ (oxidation). Thus, electrodeposition at electrolyte temperatures $T > 40\text{--}45$ °C results in Ni–Fe films with a lower concentration of iron. The absence of electrolyte mixing during electrodeposition reduces the concentration of Fe^{2+} ions in the cathode region, which also leads to a decrease in the iron content in films with small thicknesses at the initial stages of growth.

In nanostructured films consisting of individual grains, the maximum deviation from stoichiometry is observed at the grain boundaries due to the high content of defects. This can cause a significant difference in the chemical composition at the grain boundary and in the volume. The boundaries of nano-sized grains are characterized by an extremely high density of defects. In addition, when the grain size decreases, the share of their borders increases significantly in relation to the volume.

The use of pulsed electrodeposition provides the growth of the grain structure, with each grain growing within a single pulse. Reducing the pulse duration leads to a decrease in the average grain size, which will be confirmed experimentally later. A decrease in the average grain size leads to an increase in the percentage of grain boundaries and defects. The results of the chemical composition study showed that switching to pulse modes and reducing the pulse duration to $t_{\text{on}} = 10^{-3}$ s causes a decrease in the iron content, and further reducing the pulse duration to $t_{\text{on}} = 10^{-5}$ s leads to an increase in the iron content in the films. Although, for the sample obtained in the mode with the minimum pulse duration, the percentage of defects at the borders should be higher than for the samples obtained with large pulse durations, due to the reduction of grain sizes. From this, it can be concluded that the processes of increasing the iron content during the transition from DC mode to modes with a pulse duration of $t_{\text{on}} \geq 10^{-3}$ s and reducing its content during the transition to a mode with a pulse duration of 10^{-5} s have different natures. This nonlinear change is supposedly the result of a change in the growth mechanism of nanostructured Ni–Fe films using different electrodeposition modes

It can be assumed that the increase in Fe content is the result of the interaction of two competing processes (processes of repolarization in the cathode fall region and increase in nucleation centers). Nevertheless, a decrease in the Fe content for the mode with the minimum pulse duration is the result of non-equilibrium processes of electrolyte depletion by iron ions in the cathode fall region with a simultaneous increase in the number of nucleation centers.

Figure 2 shows diffractograms of Ni–Fe films synthesized with different pulse durations at 60 s of deposition, obtained by XRD. Diffractograms show two distinct peaks for three samples of films obtained by pulsed electrodeposition, while three peaks are observed for the film synthesized in DC mode. The most intense peaks correspond to the angles of ~51–52, ~59–60 and ~88–90 deg. and characterize the atomic planes (111), (200) and (220), respectively. Analysis of diffractograms showed that all the studied samples of Ni–Fe films are single-phase isostructured samples with a cubic lattice and the Fm3m (225) spatial group. With the switching from DC mode to pulse modes and with a decrease in the pulse

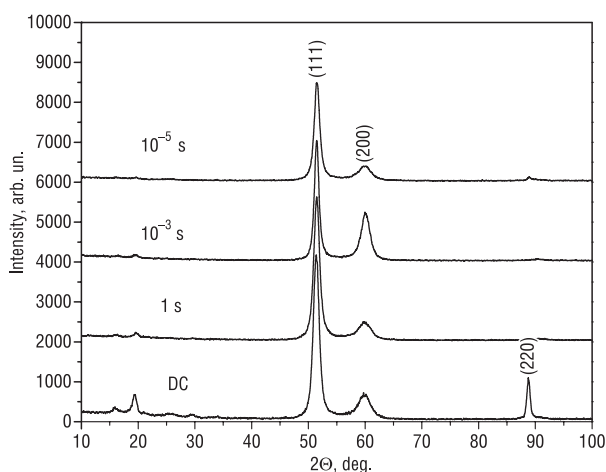


Fig. 2. Diffractograms of Ni–Fe films obtained with different pulse durations, $t_{\text{full}} = 60$ s

duration on diffractograms, there was a decrease in the intensity and an increase in the width of the peaks, which was due to the changes in the content of microdefects and to the decrease in the average size of the crystallite.

Peak corresponding to small angles ~16–19 deg. is clearly distinguishable for the film obtained in the DC mode, and switching to the pulse mode with a pulse duration of 1 s, its intensity decreases significantly. This peak is not observed in films synthesized in pulse modes with pulse durations of 10^{-3} and 10^{-5} s. This may indicate an anisotropic form and the presence of a preferred orientation of crystallites in Ni–Fe films synthesized in DC modes and in the mode with the maximum pulse duration. There is also an intense peak at angles of ~88–90 deg. that corresponds to

the atomic plane (220) and disappears with the transition to pulse modes, which confirms the isotropic shape of the crystallites and the reduction of the size of the crystallites without a preferred orientation.

Table 2 shows the main crystallographic parameters of film samples obtained in various electrodeposition modes at full deposition time $t_{\text{full}} = 60$ s. The parameter of the unit cell a and the volume of the unit cell V increase when switching to pulsed electrodeposition modes and reducing the pulse duration to 10^{-3} s, and for a sample obtained at $t_{\text{on}} = 10^{-5}$ s, a dramatic decrease in these values is observed. Thus, with an increase in the iron content from 20.61 to 24.45 at.%, the parameter of unit cell a increases from 3.553 to 3.573 Å. This is due to the larger radius of the Fe atom (1.56 Å) compared to Ni (1.24 Å). A significant decrease in the unit cell parameter a from 3.573 to 3.543 Å, observed when the pulse duration decreases from 10^{-3} to 10^{-5} , can be caused not only by a decrease in the Fe concentration in the films, but also by the influence of surface compression of the crystallites. Surface compression of crystallites is observed in nanoscale particles when the proportion of the surface layer is comparable to the proportion of the material in the volume of crystallites. Surface compression can reduce the unit cell parameter.

Table 2. Nominal chemical composition and main crystallographic parameters of Ni–Fe films obtained with different pulse durations, determined by the results of EDX and XRD

Mode	Nominal chemical composition	Unit cell parameter, a , Å	Unit cell volume, V , Å ³	Interplanar spacing, Å		
				d_{111}	d_{200}	d_{220}
DC	Ni _{79.39} Fe _{20.61}	3.553	44.852	2.0513	1.7765	1.2562
LP, $t_{\text{on}} = 1$ s	Ni _{77.86} Fe _{22.14}	3.565	45.308	2.0583	1.7825	1.2604
MP, $t_{\text{on}} = 10^{-3}$ s	Ni _{75.55} Fe _{24.45}	3.573	45.614	2.0629	1.7865	–
SP, $t_{\text{on}} = 10^{-5}$ s	Ni _{81.76} Fe _{18.24}	3.543	44.657	2.0497	1.7675	–

Figure 3 shows the evolution of the surface morphology of Ni–Fe nanostructured films at the initial stages of growth during the transition from DC to pulse modes and when the pulse duration decreases. It was found that with the transition to pulse modes and with a decrease in the pulse duration, the surface becomes more homogeneous, less porous and less defective. The film obtained in DC mode during 60 s of electrodeposition (Fig. 3, *a, b*) had a thickness of 800 ± 70 nm. On the surface there are pores with sizes from hundreds of nanometers to a few units of micrometers and conglomerates of grains with sizes from 100 to 500 nm. The average surface roughness of the Ni–Fe film synthesized in DC mode was $Ra = 17.7 \pm 0.8$ nm. With the transition to the pulse mode of electrodeposition at $t_{\text{on}} = 1$ s, the roughness decreases to the value $Ra = 11.3 \pm 0.7$ nm, and the porosity significantly declines, and the surface uniformity increases (Fig. 3, *c, d*). When the pulse duration is further reduced, the roughness value is reduced to 6.6 and 1.5 nm for the pulsed electrodeposition mode with $t_{\text{on}} = 10^{-3}$ s and $t_{\text{on}} = 10^{-5}$ s, respectively. The results of the AFM surface morphology study correlate well with the data obtained by the SEM method.

The grain size distribution for films produced in different modes is shown in Fig. 4. The most probably diameter of a single grain formed on the surface of a Ni–Fe film in DC mode is 41 nm at $t_{\text{on}} = 1$ s – 20 nm, a film with the most likely grain size of 13 nm is formed in the mode with $t_{\text{on}} = 10^{-3}$ s, and in the mode with $t_{\text{on}} = 10^{-5}$ s – 6 nm.

The decrease in the average grain size is due to a decrease in the duration of the current pulse during electrodeposition. In DC mode, the growth of Ni–Fe system crystallites is performed continuously. This is how films with a developed surface, high roughness and defects are formed. In pulse modes, at the moment of the beginning of the current pulse, an embryo is formed – the center of crystallization, on which the recovery of ions from the electrolyte solution continues for the entire time of the pulse. Grain growth stops when the current is turned off. Thus, the pulse duration determines the size of the film grains.

The surface morphology of films obtained in the mode with a minimum pulse duration of 10^{-5} s, differs significantly from the morphology of samples synthesized in other modes. There are no pores on the surface of the film. The surface is characterized by high uniformity, extremely small grain size and low roughness. The grains formed in the DC mode, long and medium pulse modes have a developed surface and a tendency to form dendrite-like structures, while the grains formed at $t_{\text{on}} = 10^{-5}$ s have the shape of an ellipsoid and form a thin continuous nanostructured film.

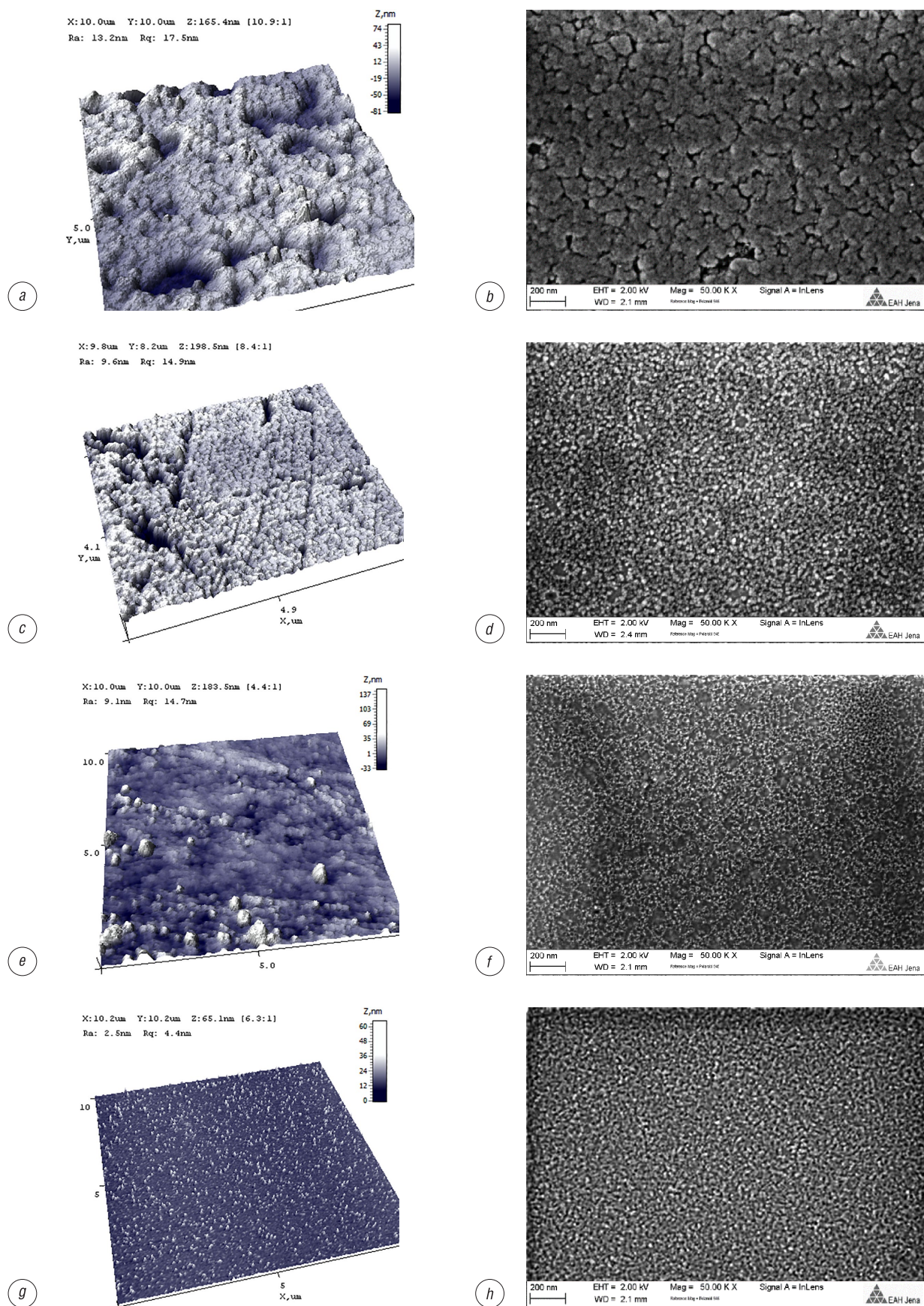


Fig. 3. Results of surface morphology study of nanostructured Ni-Fe films obtained in different electrodeposition modes using AFM (*a, c, e, g*) and SEM (*b, d, f, h*): *a, b* – DC mode; *c, d* – $t_{\text{on}} = 1$ s; *e, f* – $t_{\text{on}} = 10^{-3}$ s; *g, h* – $t_{\text{on}} = 10^{-5}$ s

The distribution of grain sizes by fractions, shown in Fig. 4, shows that films, obtained in the mode with the minimum pulse duration, have a minimum size spread of nanoscale grains. For example, during 5 s of pulsed electrodeposition in the mode with the minimum pulse duration, a film, 85 % of the grains of which are less than 10 nm in size, is formed.

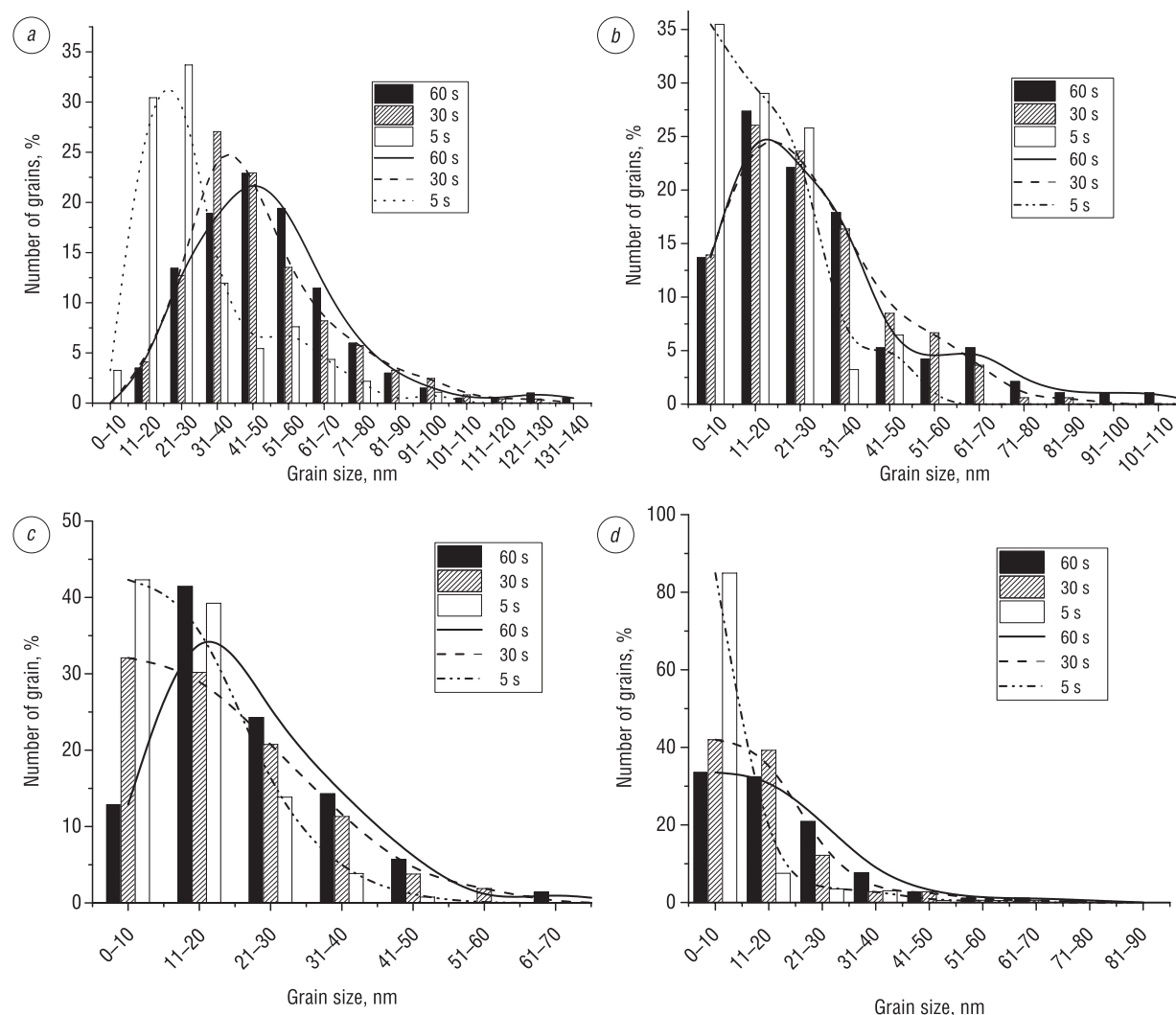


Fig. 4. Grain size distribution of thin Ni-Fe films at the initial stages of growth obtained in different electrodeposition modes: a – DC mode; b – $t_{on} = 1$ s; c – $t_{on} = 10^{-3}$ s; d – $t_{on} = 10^{-5}$ s

The diagrams of changes in the modulus of elasticity (E) and microhardness (H) (Fig. 5) show that experimental samples obtained in DC and pulse modes at $t_{on} = 1$ s and $t_{on} = 10^{-3}$ s are characterized by a close value of the modulus of elasticity, ranging from 160 to 162 GPa. Microhardness during the transition from DC mode to pulse mode increased from 6.3 to 7.2 GPa, which is a consequence of reducing the film's defects and porosity, as well as reducing the average grain size from 40 to 20 nm. When the pulse duration is reduced to 10^{-5} s, there is a significant increase in the modulus of elasticity and microhardness to 189 GPa and 10.8 GPa, respectively. Micromechanical properties are determined by the grain size and the number of grain boundaries. When switching to the mode with the minimum pulse duration, the grain size becomes less than 10 nm and the share of the interface between the grains becomes comparable to the grain volume. In addition, the density increases due to the uniformity of the surface and the cell parameter decreases – in other words, the density of the package increases, which leads to a significant increase in micromechanical properties.

Figure 6 shows the results of the study of the modulus of elasticity and microhardness under the influence of heating. Films formed in the pulse mode at $t_{on} = 10^{-5}$ s and characterized by maximum micromechanical properties were subjected to heat treatment. After heat treatment at 100, 200, 300, 400 °C, the mi-

micromechanical properties of Ni–Fe nanostructured films decreased. The change in micromechanical properties is due to the influence of many competing processes that are activated when the temperature increases. The greatest contribution is made by the processes of heterodiffusion of the sublayer material (gold) into the permalloy film, as well as intergranular diffusion, which contributes to the homogenization of the material, and recrystallization. At the same time, the surface is being oxidized.

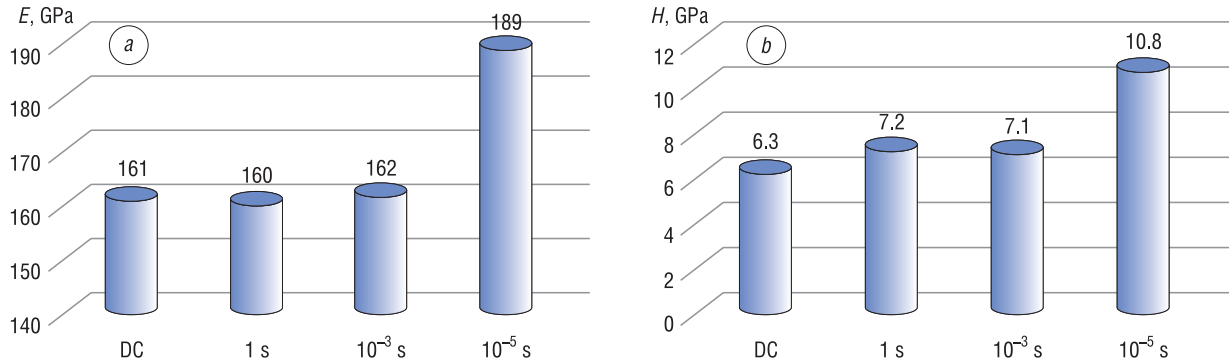


Fig. 5. Micromechanical properties of nanostructured Ni–Fe films obtained in different electrodeposition modes: *a* – modulus of elasticity, *b* – microhardness

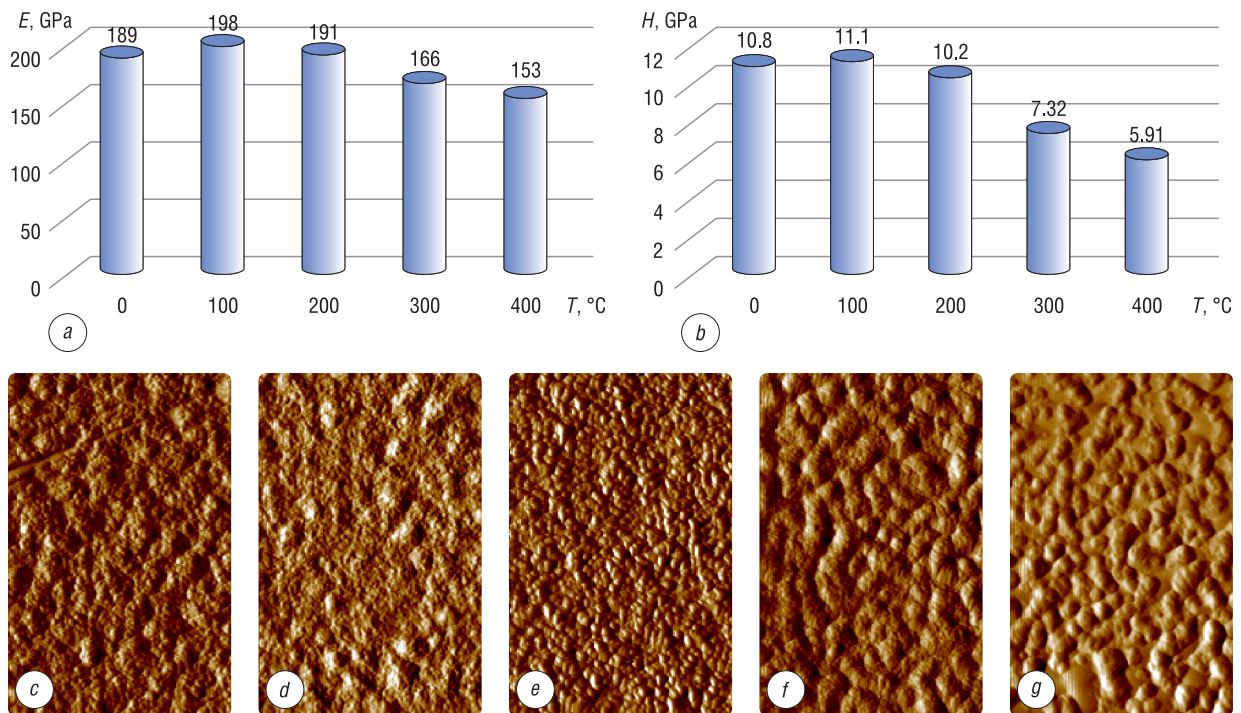


Fig. 6. Effect of heat treatment on the modulus of elasticity, microhardness and microstructure of nanostructured Ni–Fe films obtained by the pulsed electrodeposition mode at $t_{\text{on}} = 10^{-5}$ s: *a* – elastic modulus of the Ni–Fe film obtained by the pulse mode at $t_{\text{on}} = 10^{-5}$ s; *b* – microhardness; *c* – microstructure of the film without heat treatment; *d* – after heat treatment at $T = 100$ °C; *e* – $T = 200$ °C; *f* – $T = 300$ °C; *g* – $T = 400$ °C

Figure 6 shows the change in the mechanical properties and the morphology of the films surface after thermal treatment. When heated, there is a continuous increase in the grain size from 6 nm (at room temperature) to 200 nm at $T = 400$ °C. Detailed analysis of the surface structure indicates that the grain size increases due to unification, which is caused by increased mobility of atoms at the grain boundaries.

Based on the Arrhenius equation and the first Fick law, the temperature-time dependence of the heterodiffusion coefficient of the sublayer material (gold) into the Ni–Fe film was obtained. The results of the calculations are shown in table 3. Taking into account that the values of microhardness and modulus of elasticity are averaged values of the results of nanoindentation over the entire thickness of the film,

the relative concentration of gold in the Ni–Fe layer was also averaged over the entire volume. The change in microhardness and modulus of elasticity is proportional to the number of grain boundaries of the material, as well as the concentration of gold atoms diffusing from the sublayer, which is an additional source of defects.

Analysis of the results showed that heat treatment at 100 °C and 200 °C leads to a slight increase in the modulus of elasticity and microhardness by reducing internal voltages. A further decrease in H and E values is related to an increase in the concentration of gold atoms in the Ni–Fe film, which has lower micromechanical properties. The results of calculating the average relative concentration of gold atoms showed that before reaching the temperature of 300 °C, the relative concentration of gold was negligibly small.

Conclusion. Thin Ni–Fe films on the Si with Au sublayer were obtained using electrolyte deposition with different current modes: direct current and three pulsed modes with pulse duration of 1 s, 10^{-3} and 10^{-5} s. It has been established that a decrease in the pulse duration leads to a decrease in the grain size of the film, an increase in uniformity and a decrease in surface imperfection and porosity. A decrease in t_{on} to 10^{-5} s leads to the formation of grains with an average size of 6 nm. It was established that films obtained with a minimum pulse duration ($t_{\text{on}} = 10^{-5}$ s) have enhanced mechanical properties. The elastic modulus of this film was 189 GPa, and the hardness was 10.8 GPa, compared with 161 and 6.3 GPa respectively for the film obtained at constant current. It has been shown that the enhancement effect is exerted by a high number of grain boundaries in fine-grained films. This was confirmed by a study of the effect of heat treatment on micromechanical properties. It was established that after heat treatment with $T = 400$ °C, the grain size increased from 6 to 200 nm and the mechanical characteristics simultaneously decreased.

Table 3. Effect of heat treatment on the diffusion of gold atoms from the sublayer into the Ni–Fe film obtained in the pulsed mode at $t_{\text{on}} = 10^{-5}$ s

$T, ^\circ\text{C}$	Calculated diffusion coefficient, cm^2/s	Average relative concentration of gold	Average grain size, nm
20	$4.95 \cdot 10^{-30}$	< 0.0001	~ 6
100	$2.18 \cdot 10^{-24}$	< 0.0001	~ 40
200	$5.09 \cdot 10^{-20}$	< 0.001	~ 100
300	$3.56 \cdot 10^{-17}$	~ 0.12	~ 180
400	$3.32 \cdot 10^{-15}$	~ 0.36	~ 200

References

1. Milton O. *The Materials Science of Thin Films*. London, Academic Press, 2002. 794 p. <https://doi.org/10.1016/C2009-0-22199-4>
2. Zangwill A. *Physics at Surface*. Cambridge, Cambridge University Press, 1996. 327 p. <http://dx.doi.org/10.1017/CB09780511622564>
3. Hocking M. G., Vasantasree V., Sidky P. *Metal and Ceramic Coatings*. Longman Scientific & Technical, 1989. 670 p.
4. Kumar C. *Magnetic Nanomaterials*. Weinheim, Wiley-VCH, 2009. 663 p.
5. Morokhov I. D., Trusov L. I., Lapovok V. N. *Physical Phenomena in Ultradisperse Media*. Moscow, Energoatomizdat Publ., 1984. 224 p. (in Russian).
6. Suzdalev I. P. *Nanotechnology: Physical Chemistry of Nanoclusters, Nanostructures and Nanomaterials*. Moscow, URSS Publ., 2006. 592 p. (in Russian).
7. Fert A., Cros V., Sampaio J. Skyrmions on the track. *Nature. Nanotechnology*, 2013, vol. 8, no. 3, pp. 152–156. <https://doi.org/10.1038/nnano.2013.29>
8. Huang S., Beyerlein I. J., Zhou C. Nanograin size effects on the strength of biphasic nanolayered composites. *Scientific Reports*, 2017, vol. 7, iss. 1, art. no. 11251. <https://doi.org/10.1038/s41598-017-10064-z>
9. Yuan R., Beyerlein I. J., Zhou C. Coupled crystal orientation-size effects on the strength of nano crystals. *Scientific Reports*, 2016, vol. 6, iss. 1, art. no. 26254. <https://doi.org/10.1038/srep26254>
10. Guo L., Oskam G., Radisic A., Hoffmann P. M., Searson P. C. Island growth in electrodeposition. *Journal of Physics D: Applied Physics*, vol. 44, no. 44, art. no. 443001. <https://doi.org/10.1088/0022-3727/44/44/443001>
11. Zubar T. I., Sharko S. A., Tishkevich D. I., Kovaleva N. N., Vinnik D. A., Gudkova S. A., Trukhanova E. L., Trofimov E. A., Chizhik S. A., Panina L. V., Trukhanov S. V., Trukhanov A. V. Anomalies in Ni–Fe nanogranular films growth. *Journal of Alloys and Compounds*, 2018, vol. 748, pp. 970–978. <https://doi.org/10.1016/j.jallcom.2018.03.245>
12. Zubar T. I., Fedosyuk V. M., Trukhanov A. V., Kovaleva N. N., Astapovich K. A., Vinnik D. A., Trukhanova E. L., Kozlovskiy A. L., Zdorovets M. V., Solobai A. A., Tishkevich D. I., Trukhanov S. V. Control of Growth Mechanism of Electrodeposited Nanocrystalline NiFe Films. *Journal of the Electrochemical Society*, 2019, vol. 166, no. 6, D173–D180. <https://doi.org/10.1149/2.1001904jes>
13. Oliver W. C., Pharr G. M. Measurement of hardness and elastic modulus by instrumented indentation: Advances in understanding and refinements to methodology. *Journal of Materials Research*, 2004, vol. 19, no. 1, pp. 3–20. <https://doi.org/10.1557/jmr.2004.19.1.3>

14. Pavlov P. V., Khokhlov A. F. *Solid State Physics*. Moscow, Vysshaya shkola Publ., 2000. 495 p. (in Russian).
15. Gnedenko B. V. *Course of Probability*. Moscow, Nauka Publ., 1988. 447 p. (in Russian).
16. Koshkin N. I., Shirkevich M. G. Handbook of Elementary Physics. Moscow, Nauka Publ., 1982. 201 p. (in Russian).
17. Zubar T., Trukhanov A., Vinnik D., Astapovich K., Tishkevich D., Kaniukov E., Kozlovskiy A., Zdorovets M., Trukhanov S., Features of the Growth Processes and Magnetic Domain Structure of NiFe Nano-objects, *Journal of Physical Chemistry C*, vol. 123, no. 44, pp. 26957–26964. <https://doi.org/10.1021/acs.jpcc.9b06997>
18. Gong J., Riemer S., Kautzky M., Tabakovic I. Composition gradient, structure, stress, roughness and magnetic properties of 5–500 nm thin NiFe films obtained by electrodeposition. *Journal of Magnetism and Magnetic Materials*, 2016, vol. 398, pp. 64–69. <https://doi.org/10.1016/j.jmmm.2015.09.036>
19. Min Y., Akbulut M., Kristiansen K., Golan Y., Israelachvili J. The role of interparticle and external forces in nanoparticle assembly. *Nature Materials*, 2008, vol. 7, iss. 7, pp. 527–538. <https://doi.org/10.1038/nmat2206>

Information about the authors

Valeri M. Fedosyuk – Corresponding Member of the National Academy of Sciences of Belarus, D. Sc. (Physics and Mathematics), General Director, Scientific and Practical Materials Research Center of the National Academy of Sciences of Belarus (19, P. Brovka Str., 220072, Minsk, Republic of Belarus). E-mail: fedosyuk@physics.by

Tatiana I. Zubar – Ph. D. (Physics and Mathematics), Senior Researcher, Scientific and Practical Materials Research Center of the National Academy of Sciences of Belarus (19, P. Brovka Str., 220072, Minsk, Republic of Belarus). E-mail: fix.tatuana@gmail.com. <https://orcid.org/0000-0002-2225-9641>

Alex V. Trukhanov – Ph. D. (Physics and Mathematics), Leading Researcher, Scientific and Practical Materials Research Center of the National Academy of Sciences of Belarus (19, P. Brovka Str., 220072, Minsk, Republic of Belarus). E-mail: truhanov86@mail.ru. <https://orcid.org/0000-0003-3430-9578>

Информация об авторах

Федосюк Валерий Михайлович – член-корреспондент Национальной академии наук Беларуси, доктор физико-математических наук, генеральный директор, Научно-практический центр Национальной академии наук Беларуси по материаловедению (ул. П. Бровки, 19, 220072, Минск, Республика Беларусь). E-mail: fedosyuk@physics.by

Зубарь Татьяна Игоревна – кандидат физико-математических наук, старший научный сотрудник, Научно-практический центр Национальной академии наук Беларуси по материаловедению (ул. П. Бровки, 19, 220072, Минск, Республика Беларусь). E-mail: fix.tatuana@gmail.com. <https://orcid.org/0000-0002-2225-9641>

Труханов Алексей Валентинович – кандидат физико-математических наук, ведущий научный сотрудник, Научно-практический центр Национальной академии наук Беларуси по материаловедению (ул. П. Бровки, 19, 220072, Минск, Республика Беларусь). E-mail: truhanov86@mail.ru. <https://orcid.org/0000-0003-3430-9578>